Pergamon

Materials Research Bulletin, Vol. 30, No. 3, pp. 325-333, 1995

0025-5408/95 $9.50 + .00

0025-5408(94)00141-3

# METASTABLE PHASE RELATIONS AND EUROPIUM(II) LUMINESCENCE OF BARIUM HEXA-ALUMINATES PREPARED BY GEL TO CRYSTALLITE CONVERSION

T.R.N.Kutty and M.Nayak
Materials Research Centre
Indian Institute of Science
Bangalore 560 012, India.

(Received December 2, 1994; Refereed)

## ABSTRACT

Wet chemical reaction of hydrated alumina gels, $Al_2O_3.yH_2O (80<y<120)$ with $Ba(OH)_2$ gives rise to crystallites of the precursor, $Ba_{1+x}Al_{12}O_{19+x-z/2}(OH)_z .nH_2O$ where $-0.2<x<0.32$, $15<z<20$ and $5<n<9$. Thermal decomposition of the precursor above 1150°C produces monophasic hexa-aluminate, $Ba_{1+x}Al_{12}O_{19+x}$. Metastability of this nonstoichiometric phase is evident from the splitting of $(00\ell)$ reflections, on heat treatment above 1600°C, indicating the subsolidus decomposition to $0.82BaO\ 6Al_2O3$ and $1.32BaO\ 6Al_2O_3$. High resolution electron microscopy reveals extensive distribution of the blocking defects and structural intergrowths. The metastable Ba-hexa-aluminates doped with Eu(II) exhibit predominantly the 436nm emission band for all the 'x' values. No deterioration in emission intensity is noticed on long term preservation of the phosphors. Differences prevailing in literature on the phase relations in Ba-hexa-aluminates can be attributed to preparative route dependent metastability.

MATERIALS INDEX:Barium hexa-aluminates, europium(II)

## INTRODUCTION

The blue emitting barium hexa-aluminate doped with Eu(II) is a preferred constituent of phosphor blends used in tricolor fluorescent lamps. This is because of their high quantum efficiency, better maintenance and appropriate emission maximum suitably adujustable in chromaticity diagram with respect to orange-red $Y_2O_3$:Eu(III) phosphor. $BaO-Al_2O_3$ forms the 'base' system for a number of related phosphors, with the peculiar crystal chemistry and phase relations prevailing therein. Existence of hexa-aluminate $BaAl_{12}O_{19}$ was originally reported by Toropov (1). Stevels (2) observed that the compound is nonstoichiometric, having the β-alumina type structure with rather broad compositional range: $Ba_{1+x}Al_{10.67+0.75x}O_{17+x}$ $(-0.2\leq x\leq 0.35)$. Haberey <u>et al</u> (3), Kimura and coworkers

(4) as well as Mateika and Lauden (5) have demonstrated the prevalence of two distinct compounds in the place of BaO $6Al_2O_3$ with the compositions 0.9BaO $6Al_2O_3$ (Phase-I) and 1.3BaO $6Al_2O_3$ (Phase-II). Smets et al (6) have concluded that Phase-I is of β-alumina type structure, whereas Phase-II is of β′-alumina structure. One of the contributory factors for the high cost of aluminate phosphors is their exceedingly high temperature >1600°C of preparation. The low temperature chemical routes for the multinary oxide systems have been optimised by us through the earlier reported gel to crystallite (G-C) conversions(7,8). In this technique, coarse gels of hydrated alumina, $Al_2O_3.yH_2O$ is reacted with $Ba(OH)_2$, resulting in crystallites of a precursor, Ba-Al oxyhydroxide which on thermal decomposition gives rise to monophasic $Ba_{1+x}Al_{12}O_{19+x}$ $(-0.2<x<.32)$, in contrast to the prevailing literature. The phases need not necessarily be of less interest merely because they are formed metastably so long as the phosphors therefrom do not show degradation. Therefore, a detailed investigation has been taken up.

## EXPERIMENTAL PROCEDURE

The experimental procedures for the synthesis of multinary oxides through the G-C conversion have been detailed in the previous publications (7,8). Briefly, coarse gels of hydrated alumina, $Al_2O_3.yH_2O$ $(80<y<120)$ was prepared by adding $NH_4OH$ at 25°C to aqueous $Al_2(SO_4)_3$ solution until the pH was around 8. The gel, washed free of $SO_4^{-2}$ and $NH_4^+$ ions, was suspended in a flask fitted with water-cooled reflux-condenser. The air in the reactor was replaced by nitrogen. Care was taken to avoid fresh entry of $CO_2$ from atmosphere using the alkali guard-tube. The reaction was carried out for 4h with continuous stirring using a magnetic stirrer. The solid product recovered from the reactor was washed free of unreacted $Ba(OH)_2$ and dried in a desiccator. The washings were analysed for Ba after precipitating as $BaSO_4$. The dried powders were analysed by wet chemical methods. Luminescent phosphors were prepared by adding Eu(III)(aq) to aluminium sulphate solution before the precipitation of hydrated alumina gel and also by adding minor amounts of $Ca(OH)_2$ or $H_3BO_3$ to the reaction mixture during the G-C conversion. The solid products were preheated at 1150°C followed by reduction in $N_2+H_2$ atmosphere. The physical methods of characterisation were the same as those of the previous publications (7,8).

## RESULTS AND DISCUSSION

Chemical compositions of the as-prepared powders and of the calcined samples are given in Table 1. As-prepared powders are Ba-Al oxyhydroxide hydrates. Fig.1 gives the DTA/TGA tracings of two samples differing in $BaO/Al_2O_3$ ratios. The thermoanalytical curves are so very different from those of $Al(OH)_3$. The TGA curves illustrate that the compound lost weight in three steps and the corresponding DTA peaks are at around 80°, 425° and 1020°C. Evolved gas analyses in all the three steps show only $H_2O$ as the product, indicating that the thermal decompositions are either dehydration or dehydroxylation. Thermal changes below 100°C can be attributed to the loss of water of hydration. The second step around 425°C is that of dehydroxylation resulting in a modified oxyhydroxide phase with lower hydroxyl content.

TABLE-1 Chemical compositions of the products

| $BaO/Al_2O_3$ (mole) | | as-prepared | Calcined at 1150°C |
|---|---|---|---|
| Reactants | Products | | |
| 0.13 | 0.13 | $Ba_{0.75}Al_{12}O_{9.7}(OH)_{18.1}$ 6H | 0.82B6A + A |
| 0.14 | 0.14 | $Ba_{0.82}Al_{12}O_{10.5}(OH)_{17}$ 5.9H | 0.82B6A |
| 0.15 | 0.15 | $Ba_{0.9}Al_{12}O_{9.4}(OH)_{19}$ 6.4H | 0.9B6A |
| 0.17 | 0.17 | $BaAl_{12}O_9(OH)_{20}$ 8.5H | B6A |
| 0.19 | 0.19 | $Ba_{1.15}Al_{12}O_{11.4}(OH)_{15.5}$ 5.4H | 1.15B6A |
| 0.20 | 0.20 | $Ba_{1.2}Al_{12}O_{11.2}(OH)_{16}$ 5.5H | 1.2B6A |
| 0.21 | 0.21 | $Ba_{1.26}Al_{12}O_{11}(OH)_{16.52}$ 5.6H | 1.26B6A |
| 0.25 | 0.22 | $Ba_{1.32}Al_{12}O_{10.3}(OH)_{18.04}$ 5.8H | 1.32B6A |
| 0.40 | 0.30 | $Ba_{1.8}Al_{12}O_{11}(OH)_{17.6}$ 5.5H | 1.32B6A + BA |
| 0.50 | 0.38 | $Ba_{2.3}Al_{12}O_{11.2}(OH)_{18.2}$ 5H | 1.32B6A + BA |

B = BaO, A = $Al_2O_3$, H = $H_2O$, BA = $BaAl_2O_4$

This, in turn decomposes in a broad range of temperature (915-1150°C). The overall chemical reaction can be represented as:

$$
\begin{aligned}
&6Al_2O_3.yH_2O + (1+x)Ba(OH)_2(aq) \xrightarrow[\text{conversions}]{\text{G-C}} \\
&\qquad Ba_{1+x}Al_{12}O_{19+x-z/2}(OH)_z.nH_2O \\
&\xrightarrow{<100°C} Ba_{1+x}Al_{12}O_{19-z/2}(OH)_z + nH_2O \\
&\xrightarrow{<425°C} Ba_{1+x}Al_{12}O_{17.5+x}(OH)_3 + (z-3)H_2O \qquad \ldots\ldots \qquad [1] \\
&\xrightarrow{>1020°C} Ba_{1+x}Al_{12}O_{19+x} \quad [-0.2< x < 0.32]
\end{aligned}
$$

The above scheme is supported by the IR absorption spectra. As-prepared samples show strong absorption in the region 3600 to 2900cm$^{-1}$ (Fig.2), which can be attributed to O-H stretching frequencies from both $H_2O$ as well as the hydroxyl groups. The shift in stretching frequency to lower energy values (3060 and 3260cm$^{-1}$) is indicative of hydrogen bonded OH groups. The band around 1620 cm$^{-1}$ arises from water of hydration which is absent for the powder when heated above

150°C. The absorptions at 1180,1110 and 1060 cm$^{-1}$ may be assigned to the stretching frequencies (antisymmetric as well as symmetric) of $AlO_4$ and are comparable to the corresponding IR bands of silicates. The absorptions below 800cm$^{-1}$ arise from the stretching frequency of $AlO_6$, as well as the librational mode (breathing mode) of OH groups. The absorption due to the bending modes will be at frequencies much below 600 cm$^{-1}$ which presently could not be recorded. After heat treatment at 250°C, the absorptions due to molecular water, including that around 1620cm$^{-1}$ have disappeared. Absorptions arising from OH groups around 3260 and 3400cm$^{-1}$ have persisted. After calcining above 700°C, only the 3400 cm$^{-1}$ band is observed. The persistance of higher frequency OH stretching band implies that the hydrogen bonded OH groups have disappeared on heat treatment, whereas more ionic (or weakly H-bonded) hydroxyl groups are present after annealing at higher temperatures. Samples calcined above 1150°C do not show any OH stretching bands. The $AlO_4$ bands also show pronounced changes after annealing above 1150°C.

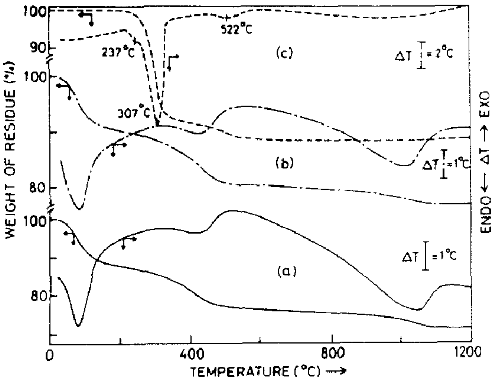

Fig.1 Simultaneous DTA/TGA tracings of the as-prepared samples having $BaO/Al_2O_3$ ratio: (a) 0.22 (b) 0.14 and (c) $Al(OH)_3$.

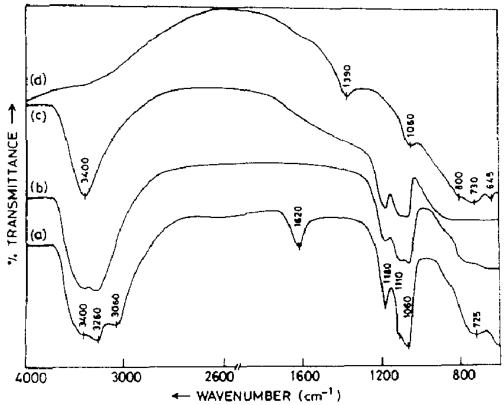

Fig.2 Infrared absorption spectra of samples with BaO $/Al_2O_3$ = 0.22 calcined at different temperatures: (a) as-prepared (b) 250°C (c) 700°C and (d) >1150°C.

X-ray powder patterns of Ba-Al oxyhydroxide (Fig.3) show complete similarity irrespective of temperature of calcining upto 1150°C. The XRD patterns do not tally with the various forms of $Al(OH)_3$ (gibbsite, bayerite, nordstrandite) or AlO(OH) (boehmite, diaspore, tohdite). The XRD tracings of samples calcined above 1150°C is so very diferent from curves (a) to (c). The curve (d) is of barium hexaalminate (Fig.3). Since the XRD patterns of Ba-Al oxyhydroxide do not tally with any known patterns, it will be indexed and reported separately.

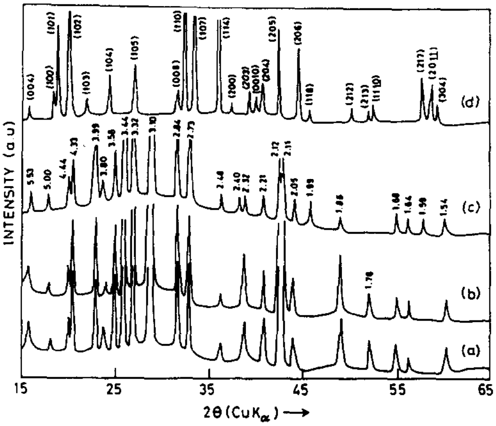

Fig.3 XRD patterns of products having $BaO/Al_2O_3$ ratio (a) 0.14 as prepared (b) 0.22 as prepared (c) 0.22 calcined at 1000°C and (d) 0.22 calcined above 1150°C.

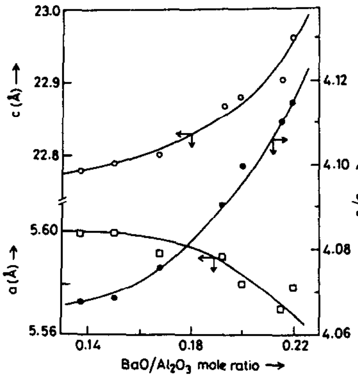

Fig.4 Variation of lattice parameters and c/a ratio with $BaO/Al_2O_3$ mole ratio.

XRD patterns of Ba-hexa-aluminates showed phase continuity irrespective of the compositional variations. Powders having Ba content lower than 0.80 (for 12 Al) show additional reflections corresponding to $Al_2O_3$. Additional reflections with low intensities corresponding to those of $BaAl_2O_4$ are noticed for samples with Ba content more than 1.32. The present observation of phase continuity, irrespective of the compositional changes is contradictory to the reports in the literature. Fig.4 reveals that a decreases with $BaO/Al_2O_3$ ratio, whereas c shows inverse relation; as a result 'c/a' ratio increases (Fig.4). These curves show no abrupt discontinuity with composition (Fig.4). According to Kimura and coworkers (4), coexistence of two phases is indicated by the splitting in (107) reflection, whereas according to Smets et al (6) splittings of (00ℓ) reflections are more diagnotic indicators of the phase multiplicity. Therefore, selected reflections were recorded under slow scanning mode for high resolution. Fig.5 gives the tracings of (107),(008) and (0010) reflections for different $BaO/Al_2O_3$ falling within the hexa-aluminate. No splitting is observed in any one of these reflections after heat treatment at 1450°C for 12 - 18h. Whereas calcining above 1650°C resulted in the splitting of (00ℓ) reflections but not (107). The intensity relations of (008) and (0010) vary as the melting temperature is approached (>1963°C). The d-spacings of the split reflections correspond to those reported for 0.9BaO $6Al_2O_3$ and 1.3BaO $6Al_2O_3$. However their intensities depend upon the initial $BaO/Al_2O_3$ ratio. Therefore hexa-aluminates prepared by gel-crystallite conversion is monophasic upto $\lesssim$ 1450°C, although the composition varied from $Ba_{0.8}Al_{12}O_{18.8}$ to $Ba_{1.32}Al_{12}O_{19.32}$ and decomposes to two phases as the temperature of annealing approaches solidus (>1963°C) in the $BaO-Al_2O_3$ phase diagram.

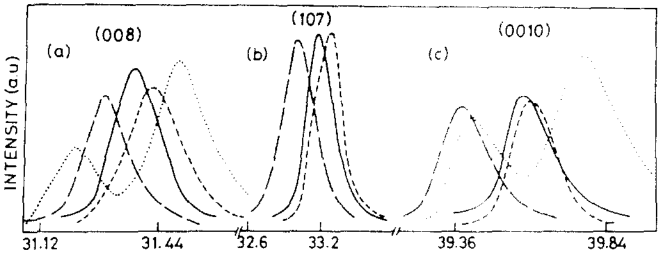

Fig.5 Selected XRD reflections of samples calcined at 1450°C with $BaO/Al_2O_3$ = 0.14(----), 0.22 (— —) and 0.19 (——). Sample calcined at 1650°C have $BaO/Al_2O_3$ = 0.19 (.....).

These results are indicative of the metastability of monophasic nonstoichiometric hexa-aluminates when prepared from low temperature routes. The decomposition of the metastable monophasic solid to stable multiphasic mixtures is thermally activated process. If the energy barrier is large enough, the subsolidus transformation will be extremely slow at lower temperatures.

Transmission electron micrographs (TEM) (Fig.6) of Ba-Al oxyhydroxide indicates that the particles were irregular shaped platelets with size ranging from 6-15nm. The electron diffraction of these particles were single crystallite spotty pattern. Particle size as well as monocrystalline nature remained, even after thermal decomposition to Ba-hexa-aluminate. The high resolution electron microscopic (HREM) study of $Ba_{1.32}Al_{12}O_{19.32}$ showed special types of extended defects (Fig.7) corresponding to'blocking defects' commonly observed in $\beta''$ -alumina structure (9). Furthermore, intergrowth features are also observable in HREM images where the changes in fringe widths at various regions are indicative of the compositional differences and the extent of ordering of Ba ions in the layers intervening the spinel blocks.

Emission spectra of Eu(II) doped Ba-hexa-aluminate has the strong band around 436nm and a weak band around 520nm, althrough the compositional range, $xBaO.6Al_2O_3$ (x=0.8-1.32) (Fig.8). Incorporation of CaO (5-15 mol%) or $B_2O_3$ (<10 mol%) drasticaly diminishes the intensity of 520nm band. This is accompanied by the increase in intensity of 436nm emission. These characteristics are unchanged with Eu(II) concentration (<5mol%). Emission intensity decreases at higher Eu(II) contents. The quantum efficiency of blue emitting phosphors containing 2mol% Eu(II) ranges from 80-86%. Eu(II) luminenescence is associated with the transition from 5d excited level to 4f ground state. The crystal field effect is, therefore, conspicuous only for the excited state whose position will depend upon covalent character of the bond between Eu(II) and the surrounding ligands. It is generally known that, Eu(II) occupying the intermediate layers between the spinel blocks in hexa-aluminates has $D_{3h}$ local symmetry. Hence the 5d level splits into A, E', E'' in the crystal field. Therefore, three bands can be expected in the excitation spectra. As seen from Fig.8 only two bands are predominent, namely 260 and 304nm. The lowest lying excitation band around 395nm reported by Stevels *et al*(10) is not discernable, although, the spectrum is asymmetric towards longer wavelengths. Fine structures in the excitation spectra depend upon the preparation conditions, thus minor diferences exist in the excitation spectrum reported by various authors (10,11). This must be arising from the metastable phase relations in Ba-hexa-aluminate system. Out of the two lattice positions associated with Eu(II) emission, the 520nm emitting is modified by the type of substitution in the spinel block. This is evident from Fig.8b, where the substitution of Ca in the octahedral sites, or B in the tetrahedral position, causes the disappearence of green band.The same changes are noticed even at higher Ba contents (Fig.9b), indicating that 520nm band is not related to Al vacancies arising out of the

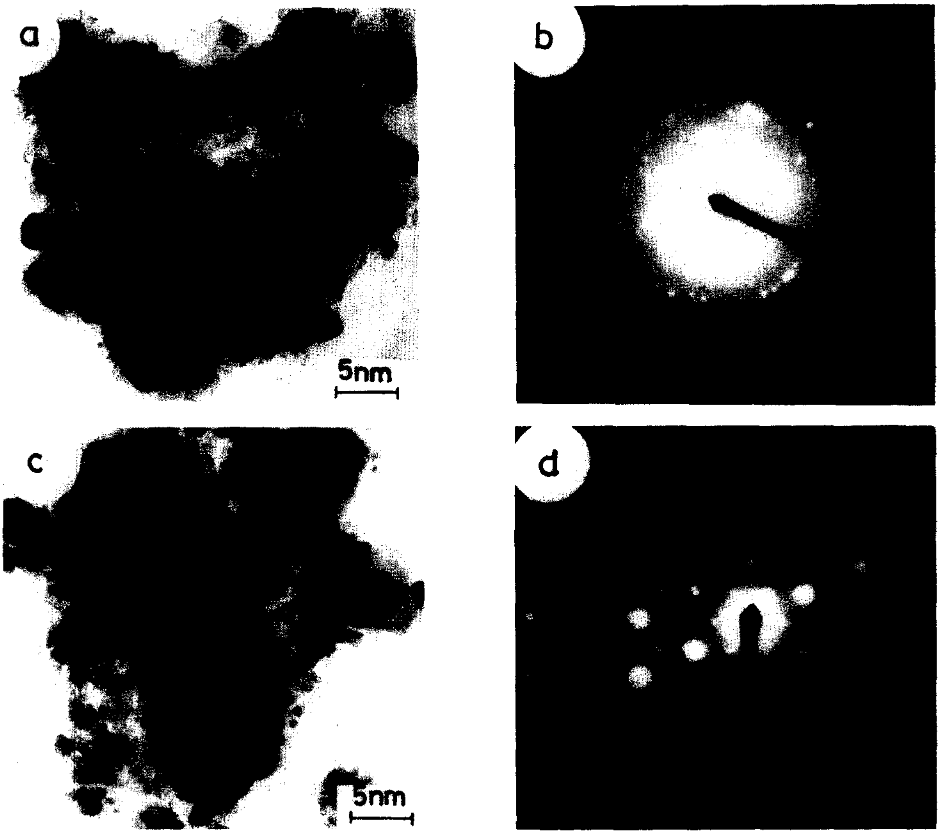

Fig.6 TEM micrographs of products having $BaO/Al_2O_3$ ratio 0.22 (a) as-prepared, (c) calcined > 1150°C, (b) and (d) are coresponding selected area diffraction patterns.

higher Ba content in the inter-block regions.The Stoke's shift in Ba hexa-aluminate is difficult to evaluate because of the uncertainity in fixing the lowest excitation band. If 304nm is considered to represent lower excitation level, Stoke's shift will be as large as 9959cm$^{-1}$. The energy transfer between Eu(II)-Eu(II) ions in hexa-aluminates is through dipole-dipole interaction, whose critical distance for energy transfer can be evaluated from the overlap between excitation and emission spectra.In the present case, the overlap is <0.08eV$^{-1}$. The critical distance calculated using the oscillator strength reported in literature(10) is~6.5 Å. Metastability does not bring about much changes in these parameters. However distinct differences prevail in the emission bands of the metastable Ba hexa - aluminate phases as compared to the spectra reported in literature. The 520nm emission is reported to be of equal intensity to that of 436nm band(6). In contrast, the 520nm emission is of minor intensity in the present case, even in samples containing lower Ba content (= 0.82 for Al). Although a common energy scheme may apply in all the cases, the concentrations of two types of Eu(II) sites are different in the biphasic as

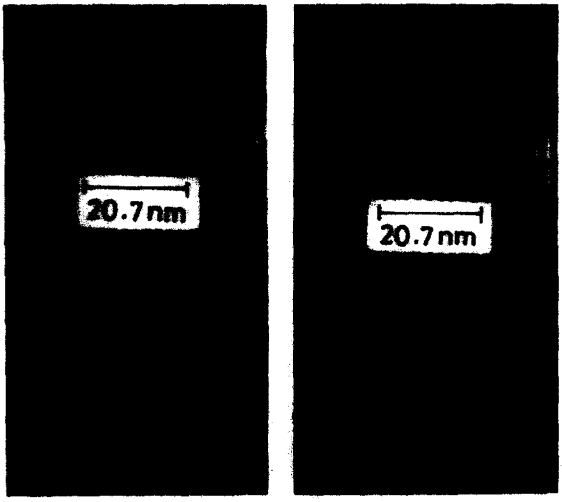

Fig. 7 HREM lattice image of 1.32BaO 6Al$_2$O$_3$ recorded with beam parallel to [100], showing (a) blocking defects (marked A) and (b) inter growth features.

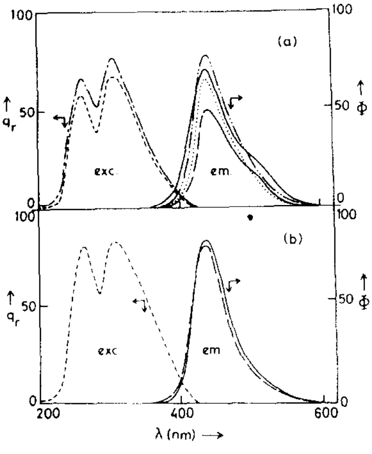

Fig. 8 Excitation spectrum (436nm emission) (----) and emission spectrum (— — $\lambda_{exc}$ = 260nm, —— $\lambda_{exc}$ = 304 nm) at 300K of 0.82BaO 6Al$_2$O$_3$:Eu(II) (a) with 10mol% B$_2$O$_3$ .... $\lambda_{exc}$ = 260 nm,—··— $\lambda_{exc}$ = 304nm and —·— $\lambda_{emi}$ = 436nm (b) with 10 mol% Ca. Φ is the radiant power per constant wavelength interval and $q_r$ the relative quantum output.

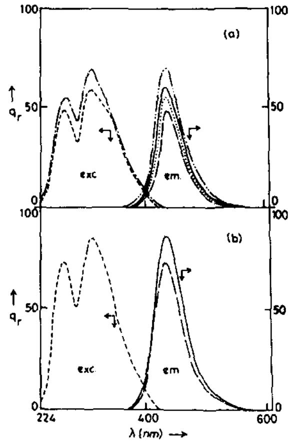

Fig.9 Excitation spectrum (436nm emission) (----) and emission spectrum (—·—$\lambda_{exc}$ = 260nm, —— $\lambda_{exc}$ = 304nm) at 300K of 1.32BaO $6Al_2O_3$, (a) with 10 mol% $B_2O_3$ .... $\lambda_{exc}$ = 304nm, —·— $\lambda_{emi}$ = 436nm (b) with 10 mol% Ca.

compared to the metastable monophasic specimens. Phosphors prepared from the low temperature G-C conversion route were preserved for extended period of 6-8 months under ambient conditions. No measurable changes were observed in photoluminescence during this period by way of shift in emission maxima nor in intensities. Since the conversion from metastable monophasic state to stable biphasic state is associated with large activation energy, alterations in luminescence features will be a minimum.

## CONCLUSIONS

The phosphors prepared from the G-C conversion route is quite efficient. Metastability does not place a limitation for the use of these phosphors as a component in tricolor lamps. Advantage of this route is that phosphors can be prepared from inexpensive water-soluble salts with procedural simplicity, bringing down the production cost. The method can be extended for the synthesis of Ba-hexa-aluminates containing other dopants such as Mn(II), Ce(III) and Tb(III).

## References

1. N.A. Toropov, Dokl. Akad. Nauk. SSSR 6,147 (1935).
2. A.L.N.Stevels, J.Lumin. 17, 121 (1978).
3. F.Haberey, G.Oehlschlegel and K.Sahl, Ber.Dt.Keram.Ges. 54, 373 (1977).
4. S.Kimura, E.Bannai and I.Shindo, Mat.Res.Bull. 17, 209 (1982).
5. D.Mateika and H.Lauden, J.Cryst.Growth. 46, 85 (1979).
6. B.Smets, J.Rutten, J.Hoeks and Verlijsdonk,J.Electrochem. Soc. 136, 2119 (1989).
7. T.R.N.Kutty and P.Padmini, Mat.Res.Bull. 27, 945 (1992).
8. P.Padmini and T.R.N.Kutty, J.Mat.Chem. 4, Dec.issue (1994) (in print)
9. J.O.Bovin, Acta Cryst. A35, 572 (1979).
10. A.L.N.Stevels and A.D.M.Schrama-de Pauw, J.Electrochem. Soc. 123, 691 (1976).
11. G.Blasse and A.Bril, Philips Res. Rept. 23, 201 (1968).